NEW INSIGHTS INTO THE MICRO- AND NANOINDENTATION OF SYNTHETIC AND BIOLOGICAL GELS

David C. Lin[1], *Emilios K. Dimitriadis*[2], *Peter J. Basser*[1] *and Ferenc Horkay*[1]

[1]Program in Physical Biology, NICHD
[2]Laboratory of Bioengineering and Physical Science, NIBIB
National Institutes of Health
9000 Rockville Pike
Bethesda, MD 20892

Introduction

Micro- and nanoindentation are common techniques in the study of the local mechanical behavior of synthetic and biological gels. In particular, the high-resolution imaging ability of the AFM has been exploited to generate localized elasticity maps of tissues and cells,[1] and even to chart the spatiotemporal evolution of stiffness during cellular processes.[2] Building on previous work in which we developed robust, automated strategies for analyzing AFM force data,[3] we introduce analytical models and approaches that further extend the capabilities of these techniques beyond the measurement of small-strain mechanical properties. These recent developments include contact equations for modeling large-strain indentation of hyperelastic materials and a method of mapping the swelling and elastic characteristics of gel samples. The refined contact equations are important in describing the indentation of many biological gels that are intrinsically nonlinear elastic, such as the cell cytoplasm and cartilage extracellular matrix. High-resolution osmotic modulus maps build on elasticity measurements to reveal swelling and volume-preservation tendencies in gels, and enhance our understanding of local inhomogeneities.

Experimental

Casting of Synthetic Gel Samples. Poly(vinyl alcohol) (PVA) gel cylinders (1 cm diameter, 1 cm height) and films (> 2 mm thick) for macroscopic displacement-controlled compression and AFM nanoindentation, respectively, were cast from aqueous PVA solution (MW 70,000-100,000; Sigma) by crosslinking with glutaraldehyde at pH ~ 1.5. An appropriate amount of crosslinker (one unit per 100 monomer units) was added to ensure that all polymer chains were attached to a continuous network structure.

Murine Articular Cartilage. Sixty-micrometer thick cartilage samples were transversely sectioned from the femoral heads of one-day old wild-type mice using a microtome. Samples were lightly fixed in 3% formaldehyde, rinsed thoroughly in PBS, and frozen in embedding medium prior to sectioning. Slices were immediately transferred to glass slides, where the embedding medium was allowed to dry and bond the tissue samples to the glass surface. The samples were then rinsed several times with a buffer solution (10 mM HEPES, 2 mM $CaCl_2$, 150 mM NaCl; pH 7.5) and equilibrated to room temperature.

Compression of Gel Cylinders. A bench top materials testing system (Stable Micro Systems, UK) was used to perform displacement-controlled compression of the PVA cylinders at a ramp speed of 1 mm/s. Volume change and barreling were visually monitored and found to be negligible. The shear modulus was determined by fitting the engineering stress-stretch data with the uniaxial hyperelastic equations listed in the first column of **Table 1**. Assuming material incompressibility, the infinitesimal Young's modulus (E_0) was then calculated by multiplying the shear modulus by a factor of three. Triplicate samples, each tested three times to ascertain elasticity, were used.

AFM Microindentation. For the synthetic gels, general-purpose silicon nitride tips with 5.5 μm glass or 9.6 μm polystyrene beads attached were used for the AFM measurements, performed using a commercial AFM (Bioscope I with Nanoscope IV controller, Veeco). Polystyrene beads of 5 μm were used for the cartilage. The spring constants of the cantilevers were measured by the thermal tune method while bead diameters were measured from images acquired during the attachment process. A raster scanning approach ("force-volume") was applied to automatically perform indentations over an area of ~ 20×20 μm, at a resolution of 16×16 (256 total indentations) for the PVA gels and over an area of ~30×30 μm at a resolution of 32×32 (1024 indentations) for the native cartilage. In all measurements, a tip velocity of approximately 814 nm/s, known from previous studies to minimize viscoelasticity in the samples, was applied. For the mouse cartilage, surface topography images were used to determine whether each measurement location corresponded to the extracellular matrix or to the cells. In the case of the engineered tissue, the dataset consisted of individual indentations acquired at random locations over the sample. An optimization approach coded in Matlab and based on the equations from **Table 1** was used to automatically process each dataset and extract values of Young's modulus.[3]

Table 1. Force-indentation Relations For Some Hyperelastic Models[1]

	Force (F) – Indentation (δ) Equation
MR NH	$F = B_1\pi\left(\frac{a^5 - 15Ra^4 + 75R^2a^3}{5Ra^2 - 50R^2a + 125R^3}\right) + B_2\pi\left(\frac{a^5 - 15Ra^4 + 75R^2a^3}{-a^3 + 15Ra^2 - 75R^2a + 125R^3}\right);\ B_1 + B_2 = \frac{20E_0}{9\pi\left(1-\nu^2\right)}$ $B_2 = 0$ for Neo - Hookean model
2p	$F = B_1\pi\left(\frac{a^5 - 15Ra^4 + 75R^2a^3}{5Ra^2 - 50R^2a + 125R^3}\right) + B_2\pi\left(\frac{a^5 - 15Ra^4 + 75R^2a^3}{5Ra^2 - 50R^2a + 125R^3}\right)\left(\frac{a^3 - 15Ra^2}{25R^2a - 125R^3}\right);\ B_1 = \frac{20E_0}{9\pi\left(1-\nu^2\right)}$
Og	$F = \frac{B\pi a^2}{\alpha}\left[\left(1 - 0.2\frac{a}{R}\right)^{-\alpha/2-1} - \left(1 - 0.2\frac{a}{R}\right)^{\alpha-1}\right];\ B = \frac{40E_0}{9\pi\left(1-\nu^2\right)}$
Fu	$F = B\pi\left(\frac{a^5 - 15Ra^4 + 75R^2a^3}{5Ra^2 - 50R^2a + 125R^3}\right)\exp\left[b\left(\frac{a^3 - 15Ra^2}{25R^2a - 125R^3}\right)\right]$ $B = \frac{20E_0}{9\pi\left(1-\nu^2\right)}$
VdW	$F = B\pi\left(\frac{a^5 - 15Ra^4 + 75R^2a^3}{5Ra^2 - 50R^2a + 125R^3}\right)\left[\left(1 - \sqrt{\frac{a^3 - 15Ra^2}{25R^2a - 125R^3}\cdot\frac{\varepsilon_m - 1}{\varepsilon_m^3 - 3\varepsilon_m^2}}\right)^{-1}\left[-b\sqrt{\frac{a^3 - 15Ra^2}{50R^2a - 250R^3}}\right]\right]$ $B = \frac{20E_0}{9\pi\left(1-\nu^2\right)}$; ε_m is the limiting tensile strain
GD TG	$F = B_1\pi\left(\frac{a^5 - 15Ra^4 + 75R^2a^3}{5Ra^2 - 50R^2a + 125R^3}\right) + \frac{B_2\pi a^2}{b}\left[\left(1 - 0.2\frac{a}{R}\right)^{-b/2-1} - \left(1 - 0.2\frac{a}{R}\right)^{b-1}\right];\ 2B_1 + B_2 = \frac{40E_0}{9\pi\left(1-\nu^2\right)}$

E_0 (infinitesimal Young's modulus), ν (Poisson's ratio), a (contact radius)
Abbreviations: MR (Mooney-Rivlin), 2p (2-term reduced polynomial), Og (Ogden), Fu (Fung), VdW (van der Waals), GD (Gaylord-Douglas), TG (Tschoegl-Gurer)

Results and Discussion

Compression and Microindentation of PVA Gels. In compression, strain stiffening of the gel cylinders was evident in the stress-stretch curves, and well-captured by each of the models listed in Table 1. The same was true in indentation, with each hyperelastic force-indentation equation yielding good fits of the AFM data and Young's modulus values comparable to those from compression. A sample fit of the compressive stress-stretch behavior for a 6% w/w gel is shown in the inset to **Figure 1**. For the 6% gels, compression yielded values of E_0 between 19.8 kPa and 20.7 kPa for the various models while indentation yielded E_0 = 18.1 – 22.9 kPa.

Microindentation of Cartilage. The main constituent of dry cartilage is type II collagen, which exists in the form of a dense network of fibrils that

forms the underlying structure of the extracellular matrix. Similar to other load-bearing soft tissues, articular cartilage has a charged nature that is responsible for its swelling behavior and compressive resistance. As essentially a compressive process, indentation provides a measure of the latter property. AFM force data showed characteristic strain stiffening in the mouse cartilage that was captured only by the Fung and Ogden equations, which are representative of exponential and power law forms of strain energy functions, respectively. **Figure 1** shows sample fits while a summary of results is presented in **Table 2**. The appropriateness of the Fung and Ogden models was expected on the basis of their demonstrated success by many researchers in describing the load-deformation behavior of various soft tissues.[4,5] In each of the two models, E_0 is a measure of stiffness at low strain while stiffening is represented by the parameters α (Ogden) and b (Fung).

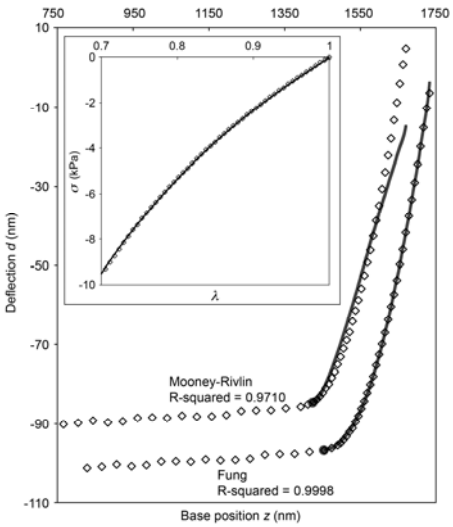

Figure 1. Sample datasets from the compression of PVA gels (inset; σ: stress, λ: stretch ratio) and indentation of cartilage extracellular matrix. Fits to the data are also shown.

Table 2. Results Of The AFM Microindentation Of Mouse Cartilage

Model	E_0 [kPa] (mean±std. dev.)	Mean R-squared
Hz	97.8±16.8	0.876
NH	99.9±19.1	0.898
MR	95.2±18.5	.0.922
2p	Failed	-
Fu	19.6±2.3	0.999
Og	19.7±3.4	0.999
VdW	96.3±18.6	0.887
GD	98.8±18.9	0.885
TG	98.0±18.8	0.885

Hz: Hertz. Data from ten randomly selected samples

Generating Osmotic Modulus Maps. In polymer physics, the osmotic modulus (K) is defined as[6] $K = c(\partial\omega/\partial c)$, where c is the polymer concentration and ω is the swelling pressure in the gel. The latter quantity is the difference between the osmotic pressure that acts to cause expansion, and the contractile elastic pressure that is represented by the shear modulus. Scaling theory predicts, and experiments have verified, that both the osmotic and elastic pressures depend on c.[6,7] We express the swelling pressure in the form $\omega = A(c^n - c_e^{n-m}c^m)$, where c_e is the concentration at the fully swollen gel and A, m, and n are constants for a particular solvent-gel combination. In a good solvent, $n = 2.25$ and $m = 1/3$.[7,8]

Osmotic modulus mapping of PVA gels in solvents of different quality revealed variations in K that were an order of magnitude larger than variations in G_0. Here, we discuss results from measurements on cartilage. **Figure 2** shows maps of the shear modulus ($G_0 = E_0/3$, assuming incompressibility) map of a cartilage sample from AFM microindentation and the corresponding osmotic modulus map. The constants $A = 4\times10^5$ kPa and $n = 2.68$ were taken from the literature for collagen gels.[9] It is evident that the local variation in K is significantly greater than the variation in G_0. It is also obvious that the influence of concentration on K is dramatically greater than on G_0. The osmotic modulus therefore serves as a better measure of the local inhomogeneity in a gel. Moreover, because K is derived from the swelling pressure, it represents the resistance to compressive deformation. Large variations in this quantity indicate significant differences in recovery from compression. This is an important consideration in articular cartilage of weight-bearing joints, which can experience large amplitude repetitive loading during physical activity and for which rapid recovery of the bulk tissue is crucial to normal function.

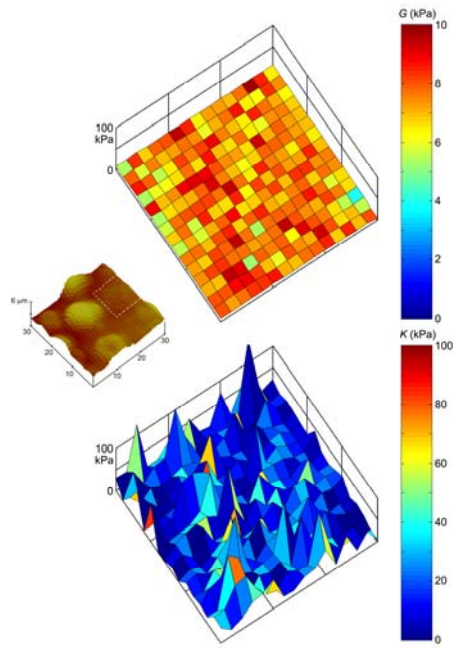

Figure 2. Shear (top) and osmotic (bottom) modulus maps of the region of extracellular matrix indicated by the dashed box in the topography map.

Conclusions

Recent developments in the indentation of gels allow us to better understand their load-deformation and swelling behavior. This is of great significance in the study of biological tissues, whose inhomogeneity is manifested across different length scales. The two advances introduced here enable us to exploit the high-resolution capabilities of the AFM in studying the properties of gels at the local level.

Acknowledgements. This work was supported by the Intramural Research Program of the NIH, NICHD.

References

(1) Lin, D.C.; Shreiber, D.I.; Dimitriadis, E.K.; Horkay, F. *Biomech. Model. Mechanobiol.* In press.
(2) Almqvist, N.; Bhatia, R.; Primbs, G.; Desai, N., Banerjee, S.; Lal, R. *Biophys. J.* **2004**, *86*, 1753.
(3) Lin, D.C.; Dimitriadis, E.K.; Horkay, F. *J. Biomech. Eng.* **2007**, *129*, 430.
(4) Maikos, J.T.; Eias, R.A.; Shreiber, D.I. *J. Neurotrauma* **2008**, *25*, 38.
(5) Pandit, A.; Lu, X.; Wang, C.; Kassab, G.S. *Am. J. Physiol. Heart Circ. Phsiol.* **2005**, *288*, H2581.
(6) Horkay, F.; Zrinyi, M. *Macromol.* **1982**, *15*, 1306.
(7) DeGennes, P.G. *Scaling Concepts in Polymer Physics* **1979**, Cornell University Press, Ithaca.
(8) Treloar, L.R.G. *The Physics of Rubber Elasticity* **1975**, Oxford University Press, Oxford.
(9) Stein, A.M.; Vader, D.A.; Weitz, D.A.; Sander, L.M. *arXiv* **2008**, 0807.2805.